Microchim Acta (2013) 180:1443–1452
DOI 10.1007/s00604-013-1095-3

ORIGINAL PAPER

Molecularly imprinted polystyrene–titania hybrids with both ionic and π–π interactions: a case study with pyrenebutyric acid

Roman Selyanchyn · Seung-Woo Lee

Received: 21 October 2012 / Accepted: 24 September 2013 / Published online: 5 October 2013

Abstract We present hybrid films consisting of a composite prepared from polystyrene (PS) and titanium dioxide (titania; TiO_2) and molecularly imprinted with 1-pyrenebutyric acid (PBA). The interaction of PBA with the polymer is shown to occur via binding of the carboxylic group to TiO_2 and hydrophobic interaction of the pyrene moiety with the PS network. We investigated the effects of the PS fraction on morphology, imprinting properties, and guest binding. The template could be completely removed by incubating the films in an acetonitrile solution of pyrene, which is due to the stronger π–π interaction between PBA and pyrene than the interaction between PBA and its binding site. A guest binding study with pyrene, 1-aminopyrene, pyrenemethanol, and anthracene-9-carboxylic acid showed that the hybrid films possessed selectivity and much higher binding capacity for PBA. This study demonstrates the first case of clear PS-assisted imprinting, where the π–π interaction of the template with a linear (non-crosslinked) polymer creates selective binding sites and enhances the binding capacity. This is a driving force for guest binding in addition to the interaction of the template/analyte with TiO_2. All molecularly imprinted films displayed better binding, repeatability and reversibility compared to the respective non-imprinted films.

Keywords Molecular imprinting · Titanium dioxide · Polystyrene · 1-pyrenebutyric acid

Electronic supplementary material The online version of this article (doi:10.1007/s00604-013-1095-3) contains supplementary material, which is available to authorized users.

R. Selyanchyn · S.-W. Lee (✉)
Graduate School of Environmental Engineering,
The University of Kitakyushu, Kitakyushu 808-0135, Japan
e-mail: leesw@kitakyu-u.ac.jp

Introduction

In general, molecularly imprinted polymers (MIP) are synthesized via three dimensional co-polymerization of functional and crosslinking monomers in the presence of a template molecule that is considered as a "recognition target" in future applications [1]. In such a system, the functional groups of monomers are spatially arranged by covalent, non-covalent, or other types of chemical interactions with the template molecules. Depending on the type of matrix material, molecular imprinting (MI) can be classified into two branches on the basis of the matrix used for imprinting i.e., organic and inorganic MI.

Although the MI with organic polymers represents the vast majority of modern research, among inorganic materials, imprinting with titanium dioxide has several advantages. Titania (and its precursors) may bind a variety of template molecules through not only carboxylate binding sites but also other functional sites that are capable of forming hydrogen bonds [2]. In the case where TiO_2 is present in the crystalline anatase or rutile forms, it can serve as an effective photocatalyst because of the specific absorbance in the UV–vis range [3, 4]. On the other hand, thick titania coatings can lack flexibility and possess slow diffusion properties.

Polystyrene (PS) represents an inexpensive polymer material that is environmentally friendly, recyclable, and widely used in a variety of applications. The advantages of polystyrene over other materials include bacterial and moisture resistance and its insulating properties. Because of the presence of the only one double bond in the styrene monomer, this linear polymer is not used for the synthesis of organic MIPs; however, to the best of our knowledge, only one study by Hsu et al. [5] successfully used styrene as a functional monomer for the surface imprinting of the RNAse A. The authors have shown that MIPs composed of styrene/PEG400DMA (20/100, v/v) had a higher rebinding capacity than materials composed of

only crosslinking agents, and suggested the role of styrene for epitopic recognition.

Hybrid composite materials of PS and titania have been widely studied for many emerging applications. In most cases, PS, used as specific templates (e.g., spheres) for the preparation of hierarchically ordered titania structures, is sacrificed by the thermal decomposition [6, 7]. Core-shell PS/TiO_2 and hollow sphere porous titania materials obtained by post-process PS removal are promising for a variety of industrial applications such as enhanced photocatalysis [8], electronic ink [9], creation of macroporous photonic crystals in titania [10], and anodes for lithium ion batteries [11]. Thin film PS/TiO_2 composites are good candidates for coatings with modulated hydrophobicity and can be switched from super hydrophilic to super hydrophobic [12–14]. In addition, novel applications of PS/TiO_2 hybrids include its use for solid-phase extraction of amino acids from biological samples [15]. In general, for preparation of these composite materials, nanostructured PS and/or TiO_2 are used, e.g., micro- or nanoparticles, nanorods, and nanocrystal powder, to achieve a symmetric hierarchical structure or ordered films with certain properties.

Recently, we demonstrated a phenomenon of well-organized phase separation between titania and polystyrene in thin films prepared via spin coating [16]. The variation of polystyrene ratio leads to its specific distribution in the film and PS can be present as a film, network, or uniformly distributed nanodots. As shown by Schmidt et al., the addition of a linear polymer to the organic MIP pre-polymerization mixture [17, 18] leads to controlled phase separation between the components, enhancing the binding properties in the films fabricated via spin coating. In the present work, by extending the applicability of nanosandwich TiO_2/PS/TiO_2 films introduced in our previous report [16], we demonstrate the phenomena of imprinting in such composite PS–titania matrix. 1-Pyrenebutyric acid as a model template for imprinting in the composite matrix possesses two different moieties providing, as suggested, two-point binding possibility where carboxylic group interacts with titania while the pyrene moiety interacts with the PS matrix. Quite selective and dense imprinting was obtained with binding parameters depending on the ratio of PS. Moreover, the morphology of the spin-coated imprinted hybrid films was studied to investigate the mechanism of film formation in the presence of the template.

Experimental

Materials and film preparation

Polystyrene (PS, monomer M_W=104.15 g • mol^{-1}), titanium (IV) tetrabutoxide (Ti(O^n-Bu)$_4$, TTBO, M_W=340.32 g • mol^{-1}), chloroform, ethanol, acetonitrile (ACN), 1-pyrenebutyric acid (PBA, M_W=288.34 g • mol^{-1}), pyrene (PYR, M_W=202.25 g • mol^{-1}), pyrenemethanol (M_W=232.28 g • mol^{-1}), 1-aminopyrene (M_W=217.27 g • mol^{-1}), and anthracene-9-carboxylic acid (9-AC, M_W=222.24 g • mol^{-1}) were purchased from commercial sources and used without additional purification. Stock solutions of 200 mM PS, 200 mM TTBO, and 200 mM TTBO complexed with 10 mM PBA in $CHCl_3$ were prepared, and were used to prepare precursor solutions with certain molar contents for individual components by adjusting the concentration of PS using pure chloroform. Totally, 11 different films were prepared by spin coating using the precursor solutions, as listed in Table 1.

The following spin-coating conditions were applied for film preparation. Silicon wafers (~4 cm^2) or transparent quartz (~2 cm^2) were used as substrates; they were washed in ethanol and water and plasma treated for 4 min (Covance-MP, Femto Science, femtoscience.co.kr, Korea). A precursor solution amount of 50 μL·cm^{-2} was placed on the silicon wafer, and then, it was rotated at a speed of 3,000 rpm. Spin coating was performed using a K-359SD-1 device (Kyowa Riken, www.kyowariken.co.jp, Japan) under nitrogen atmosphere. To complete hydrolysis, the TTOB films were maintained in normal humidity at room conditions for 24 h before the first usage.

Film characterization

The morphology of surfaces and cross-sections of the prepared films were investigated by optical microscopy (OM; Suruga Seiki M331 micromanipulator assembled with Sony 3CCD Exwave HAD camera, www.suruga-g.co.jp, Japan), fluorescence microscopy (FM; SteREO, Lumar. V12, Zeiss, microscopy.zeiss.com, Germany), scanning electron

Table 1 Concentrations of each component in the hybrid film precursor solutions

	Notation in text	TTBO in precursor, mM	PS in precursor, mM	PBA in precursor, mM
Imprinted films				
MI-100:100:5	MI-100	100	100	5
MI-100:80:5	MI-80		80	
MI-100:60:5	MI-60		60	
MI-100:40:5	MI-40		40	
MI-100:20:5	MI-20		20	
MI-100:10:5	MI-10		10	
MI-100:5:5	MI-5		5	
MI-100: 0:5	MI-0		0	
Non-imprinted films				
NI-100:100:0	NI-100	100	100	0
NI-100:20:0	NI-20		20	
NI-100:0:0	NI-0		0	

microscopy (SEM, CarryScope S5700, JEOL, www.jeol.com, Japan), and field emission scanning electron microscopy (FESEM, Hitachi S-5200, www.hitachi.com, Japan). Before the SEM measurements, the films were vacuum-dried for 6 h to thoroughly remove solvent and water molecules adsorbed on the films, and thereafter they were coated with a thin (ca. 5 nm) platinum film using an ion sputter (15 mA, 10 Pa, Hitachi E-1030, www.hitachi.com, Japan) to avoid electrical charge-up of the sample surface by the electron beam.

Template removal was confirmed by UV–vis–NIR spectroscopy (V-570 UV–vis spectrophotometer, JASCO, www.jascoint.co.jp, Japan) of the films deposited on the quartz plates. In addition, reflectance interference spectroscopy (RIfS) performed with a conventional set-up (UV–vis–NIR light source DH-200-BAL, spectrometer S1024DW, and R400-7 fiber optic probe, all Ocean Optics, www.oceanoptics.com) was used to confirm the film uniformity and characterize template incorporation and removal.

Template removal and guest binding

Template removal from the prepared films was performed by two different methods. The first method followed the conventional approach based on the cleavage of the carboxylate bond to the titania matrix, i.e., conditioning in 0.1 wt.% ammonia [2, 19–24] for 30 min. The second method involved short term conditioning (~10 min) of the films in 3 mM neutral pyrene solution in ACN. The guest binding of PBA and other compounds was conducted using an acetonitrile solution of the guest molecule (basic concentration maintained at 3 mM in ACN). Specific absorbance changes due to the template removal and rebinding were monitored by UV–vis spectrometry or RIfS.

For selectivity tests, the binding of several structurally similar compounds such as pyrene, pyrenemethanol, 1-aminopyrene, and antracene-9-carboxylic acid to the imprinted films was tested. The structures of the template molecule and other compounds are provided in ESM Fig. S1. The binding of all compounds was conducted under similar conditions; namely films were incubated in 3 mM guest molecule solution in ACN for 40 min. After incubation, thorough washing in ACN followed by washing in water was conducted, and finally, the film was dried in a stream of nitrogen gas.

Results and discussion

Structural characterization of the MIP films

Optical microscopy and reflectance measurements

The OM measurements of the fabricated films together with RIfS analysis provided information about the film structure and elucidated changes that took place after the PBA template was removed from the film. Figure 1 shows the surface of the films depending on the PS content before and after template removal. Significant changes were observed even in the macromorphology of the films with PS contents of 40 mM or higher. When the PS concentration in the precursor solution was 5, 10, or 20 mM, it was not sufficient to form a network and the polymer was present in the form of uniformly distributed domains covered by a TiO_2 film. At higher PS contents, these domains started to form a network that became denser with increasing amount of PS. The OM investigation of the film surface showed that no changes were observed before and after template removal when 0.1 wt.% ammonia washing was used to remove the template.

On the other hand, the RIfS investigation of the films deposited on the silicon wafer enabled the assessment of the morphological uniformity (film thickness and structure) of the film by comparing the reflectance spectra in different places of the film. In addition, this method allowed us to check the presence of PBA in the film after preparation (to confirm successful incorporation) and after washing with ammonia (to confirm template removal). Figure 2 shows the reflectance spectra of three different MI films before and after template removal. It is observed that for pure titania (MI-0), ammonia washing was sufficient to remove the entire template, while there was template residue visible in the MI-100 film. The PBA absorption peak at around 350 nm was not completely removed, indicating the presence of template residue. For MI-20, the peak almost disappeared, but the presence of small plateaus near 350 nm shows a little residue of the template. These results demonstrate that the template has a different binding feature in the films with PS and cannot be removed thoroughly by conventional ammonia washing. The error bars in the insets of Fig. 2 show the variation of the RI spectra measured at different locations on the film, indicating high uniformity of the films in terms of thickness and structure.

On the basis of the OM results, particularly those in Fig. 1, we can conclude that similar to our previous work [16], three types of phase separated structures were formed depending on the content of PS in the film. At concentrations equal to or higher than 40 mM in the precursor solution, PS forms networks in the film with an l layer being formed at a concentration of 100 mM. In contrast, at lower concentrations, PS is present in the form of uniformly dispersed dotted domains. Thus, to describe the features of the films, three representative conditions were selected and further investigated: PS = 100 (film, network), PS = 20 (dotted domains), and PS = 0 (conventional TiO_2 film).

In the case of template removal by washing in 3 mM pyrene in ACN, significant changes in the films with PS were found when observed by OM, whereas the same changes were not observed in the NI films (see Fig. S2 in ESI). Namely, for MI films with PS, the initially present interference colouring disappears, indicating a change in the film structure. In

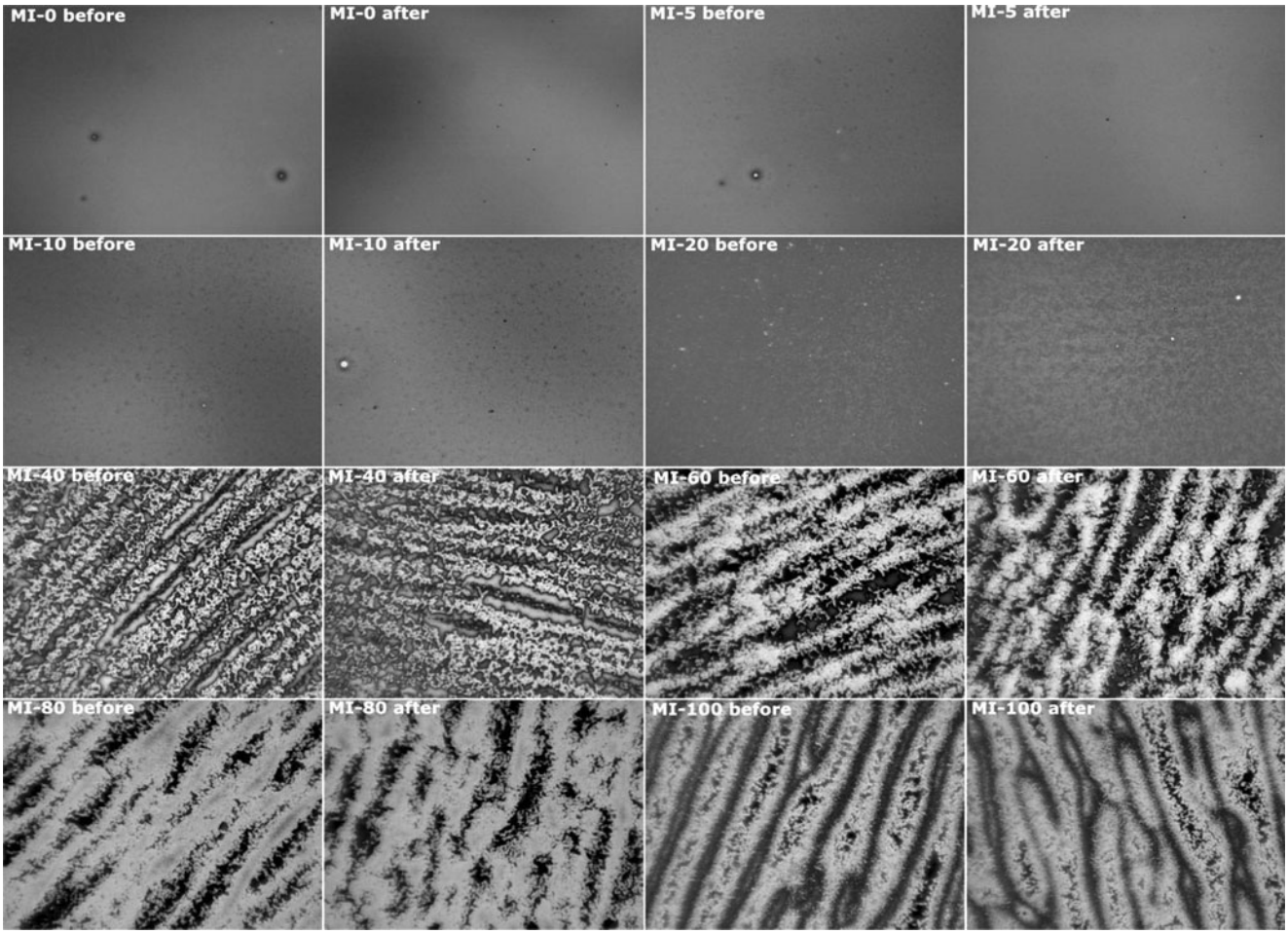

Fig. 1 Optical images of the MI-X films before and after PBA template removal by ammonia washing (X: actual content of the PS in the initial solution indicated in each figure)

addition, the films conditioned in 3 mM pyrene in ACN were no longer measurable by RIfS, indicating that the film structure underwent a significant morphological change. As all these changes were not observed by OM because of its low resolution, SEM investigations were undertaken as a further step of film characterization.

SEM investigation

The phenomena of phase separation between the titania and PS components, introduced in our previous work [16], satisfactorily explain the structural features of the MI films, as can be seen from the SEM images of Fig. 3. For MI-100, PS forms networks between the layers of titania (Figs. 3a and e), whereas for MI-20, it is present in the form of small clusters (~400 nm) covered by titania (Fig. 3b). In addition, the SEM investigation of the MI films revealed structural transformations after conditioning in 3 mM pyrene in ACN. In both cases, the PS domains appear to be shrunken because of their clearly phase-separated surfaces after template removal (Figs. 3c and d).

The cross-sectional SEM images of the fabricated MI films are shown in Figs. 3e and f, demonstrating that the difference in the thickness is significantly dependent on the PS content. The MI-100 film is almost three times thicker than the MI-20 film before template removal, and perhaps, this increase in thickness can be attributed to the higher PS content.

These observations of the film surfaces are important for explaining the complete removal of PBA after conditioning in ACN with pyrene, the disappearance of the interference patterns, and the disturbance of the reflectance spectra (data not shown). The PBA template that has been complexed with the TiO_2 matrix is probably present in two different forms inside the film: one part is covered by pure titania matrix and the other is additionally surrounded by the PS matrix. The conventional ammonia treatment is sufficient to remove the former from the film but the latter will need a more specific process for template removal. It appears that the conditioning using pyrene in ACN is useful to extract the template that was bound to the film through the hydrophobic interaction of the pyrene moiety with the PS polymeric networks, in addition to the ionic bond with the TiO_2 matrix. As a result of template removal, PS lost the

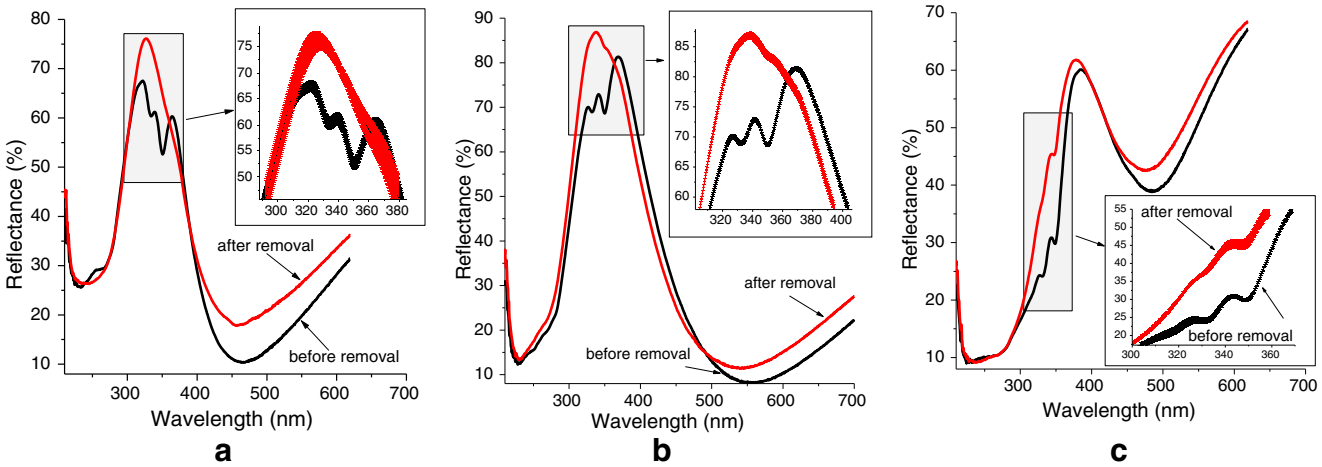

Fig. 2 Reflectance interference spectra of the MI films with ((**a**) PS = 0, (**b**) PS = 20, and (**c**) PS = 100) before and after template removal by washing with 0.1 wt.% ammonia. The inset figures show enlargements of the enclosed parts of the RI spectra with PBA absorption feature (peaks at around 350 and 330 nm)

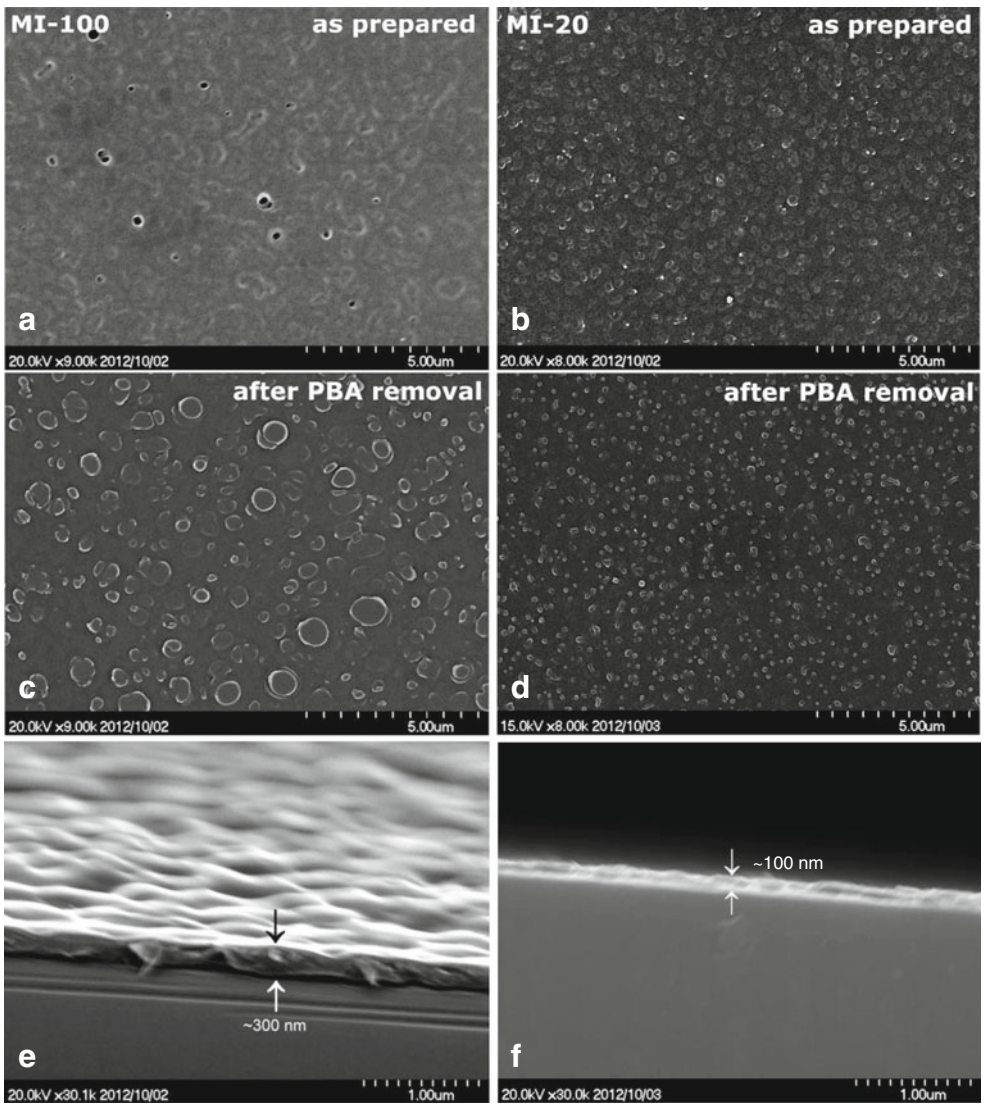

Fig. 3 SEM images of the MI-100 and MI-20 films surfaces before (**a** and **b**) and after (**c** and **d**) PBA extraction by a 3 mM solution of pyrene. The cross sections of the as-prepared (**e**) MI-100 and (**f**) MI-20 films

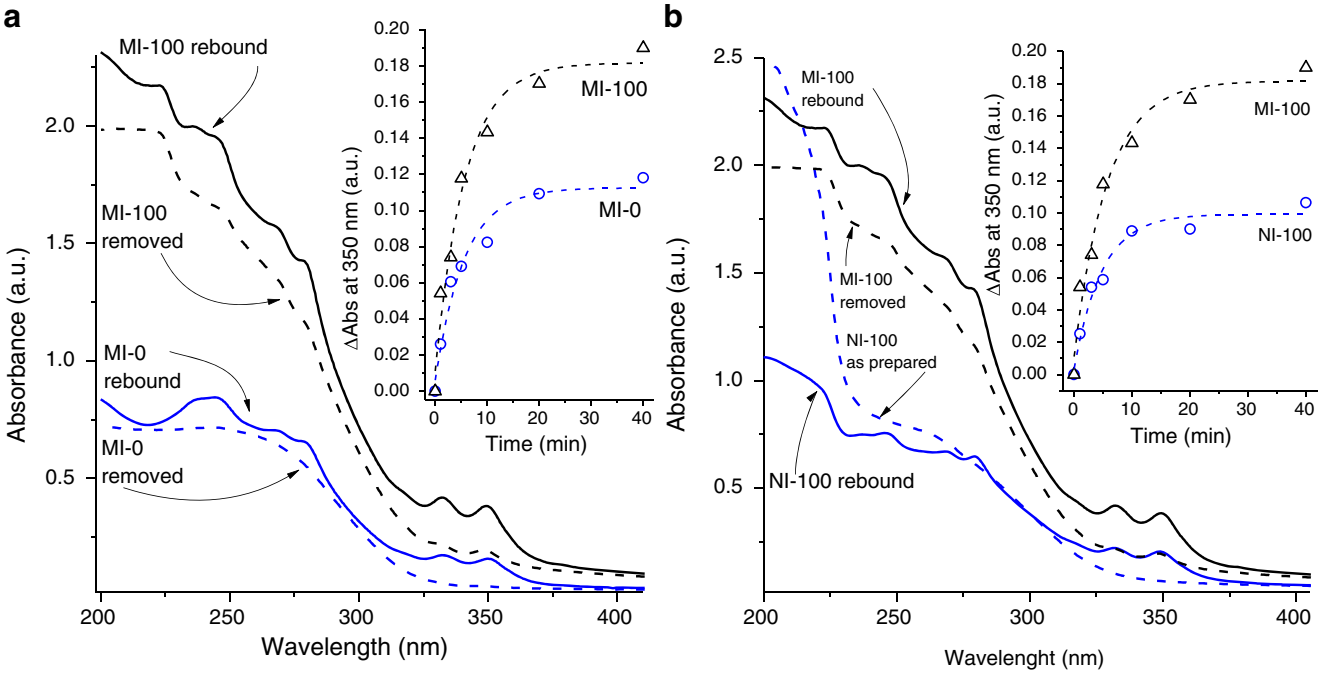

Fig. 4 Template rebinding in the films: (**a**) MI-100 compared with MI-0 and (**b**) MI-100 compared with non-imprinted film NI-100 (PBA = 0). PBA binding was conducted using 3 mM PBA in ACN

template-mediated connection with titania and was slightly shrunken (MI-100) or produced nanocracks (nanoholes) around the domains, as shown in Fig. S4b for MI-20. However, these morphological changes do not change the imprinting properties (as will be shown later), and moreover improve them because of increased film permeability.

Template removal and rebinding

As mentioned in the experimental section, we have tried two different methods of template removal from the films. In general, 0.1 wt.% ammonia is sufficient for quick removal of the carboxylic templates embedded in titania [21], and for MI-0, it was enough to remove the PBA template completely. However, some residual template was still observed in films including PS, for both MI-20 and MI-100, with more residue in the latter case.

Figure 4 shows the UV–vis spectra of the films deposited on quartz plates after removal and rebinding of the PBA template, where the original spectra are not shown here because they are similar to their "rebound" curves. The insets of both graphs in Fig. 4 show the dynamics of template removal by incubation in 0.1 wt.% ammonia. It is observed that the absorbance change at 350 nm reaches saturation after ca. 20 min. Thus, we conditioned the films in 0.1 wt.% ammonia

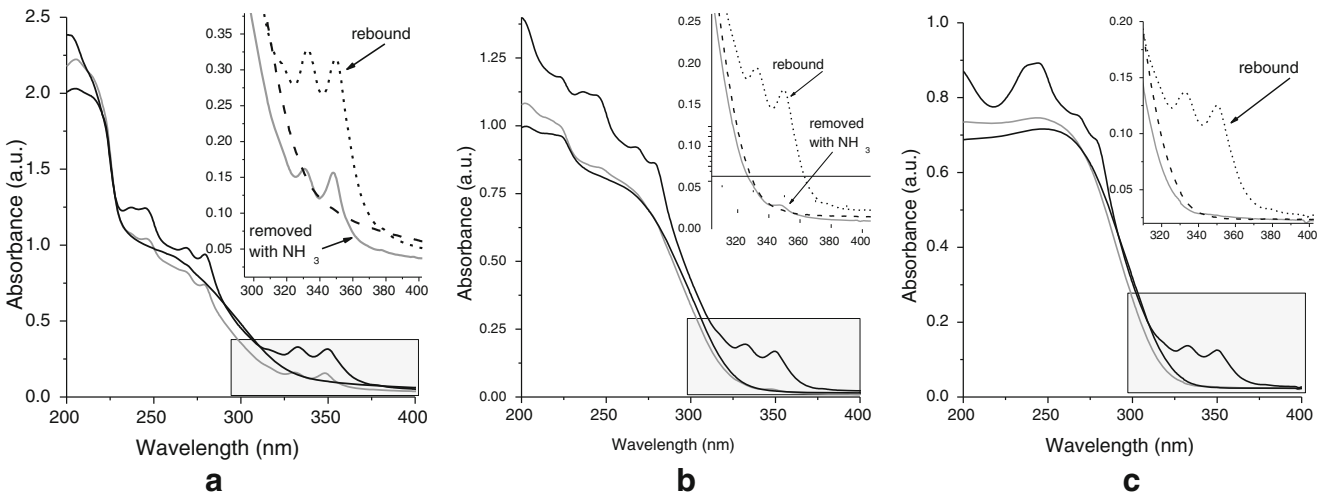

Fig. 5 Template rebinding (*short dashed line*) and removal with 0.1 wt.% aqueous ammonia (*solid grey line*) or 3 mM pyrene in ACN (*long dashed line*) for the imprinted films: (**a**) MI-100, (**b**) MI-20, and (**c**) MI-0

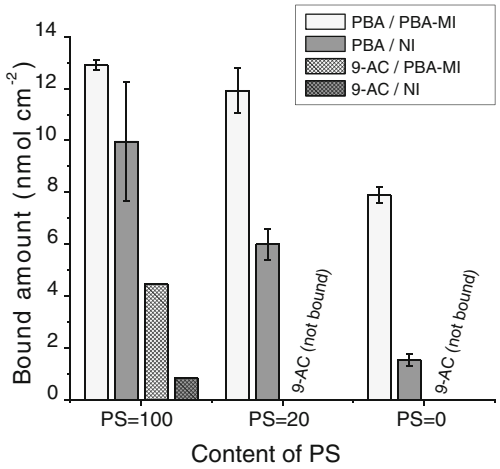

Fig. 6 Amount of bound guest molecules for the imprinted and non-imprinted films (pyrene, 1-pyrenemethanol, and 1-aminopyrene were not bound to any of these films—data not shown)

for 30 min in the further tests for PBA removal. Interestingly, we achieved complete rebinding of the template to the film in all cases by incubating the films in the 3 mM PBA template, by comparing the original UV–vis spectrum of the film (after fabrication) and that of the film after rebinding.

On the other hand, after PBA rebinding in ACN, the UV absorption of the NI-100 film at around 200 nm, which is attributed to the phenyl ring moiety of PS, drastically decreased, whereas its absorption peaks at around 260 nm show similar to those of the MI-0 film. Perhaps, this indicates that most parts of PS were removed from the film by the treatment of PBA in ACN, revealing an adhesive instability between PS and titania inside the film.

The phenomenon of the template removal by incubation in the 3 mM ACN solution of neutral pyrene was discovered during the selectivity tests. When pyrene was used as a guest to the imprinted material, we observed complete removal of PBA from all MI films. The UV–vis spectra of the three different films presented in Fig. 5 show three different conditions for : (1) rebinding, (2) removal with ammonia, and (3) removal with 3 mM pyrene in ACN. After the conditioning in the pyrene solution, no specific absorption peaks that can be attributed to the PBA template or pyrene were observed. Thus, we conclude that due to the possible π–π interaction between neutral pyrene and PBA (e.g., excimer state formation), residual PBA, not removed by ammonia, was stacked to pyrene and successfully removed from the film. This observed phenomenon that 3 mM pyrene in ACN can remove the template and does not destroy the binding site was validated by multiple rebinding tests. In further tests, this method was used to remove the template instead of conditioning in an aqueous NH_3 solution. Moreover, the time required for removal was shorter, and for further tests, 10 min incubation in 3 mM pyrene in ACN was sufficient for complete removal of the bound guest molecules. Interestingly, the incubation of the film in pure ACN for a period of up to 1 h could not remove the bound PBA from the fabricated films (Fig. S7 in ESM). This indicates that the removal of bound guest molecules cannot be attributed only to the action of ACN.

Selectivity tests

In addition, selectivity tests with the four different compounds were conducted. The films showed binding to anthracene-9-carboxylic acid (9-AC) and did not show any binding to pyrene or 1-aminotpyrene. Only trace amounts of binding of some films to pyrenemethanol were observed. Figure 6 shows different amounts of bound guest molecules per square centimeter from the 3 mM solution in ACN for six different types of films (three imprinted and three non-imprinted). Interestingly, little binding of 9-AC was observed only in the PBA imprinted film with PS = 100, suggesting that this binding was achieved solely because of PS and not titania. Higher selective binding was achieved in the MI-20 and MI-0 films. This result provides a valuable tool for increasing the binding capacity without sacrificing selectivity. A higher level of binding of PBA was

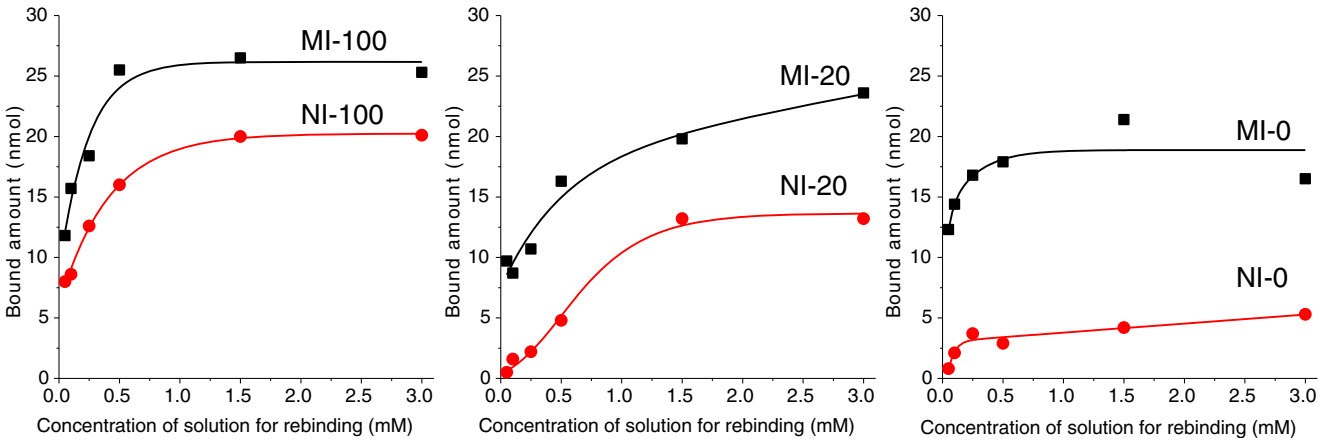

Fig. 7 Binding isotherms for the binding of PBA on the PBA-imprinted (*black lines*) and non-imprinted (*red lines*) TiO_2/PS hybrid films

Table 2 Binding constant and maximum bound amount for the fabricated films

Film type	K_D	N_{max}, nmol·cm^{-2}
MI-100:100:5	0.093	14.1
NI-100:100:0	0.156	10.3
MI-100:20:5	0.172	11.5
MI-100:0:5	0.032	8.9

obtained in the MI-100 film, but the possibility of non-selective binding also appears probable. To summarize, for this particular system of template and polymer, the best selectivity was obtained for pure titania films and increasing the polystyrene content significantly decreased the selectivity. However, optimizing the content of PS may provide benefits in such systems, e.g., for the MI-20 film, where selectivity is similar but the maximum bound content is larger.

Binding constant determination tests

If a 1:1 stoichiometry of the complex is assumed, the dissociation constant K_D between the guest (G) and binding site (BS) in the molecularly imprinted polymer can be defined by Eq. 1 [25].

$$G + BS \overset{K_D}{\longleftrightarrow} G/BS \tag{1}$$

with K_D defined as given by the Eq. 2,

$$K_D = \frac{N_{unbound}}{N_{bound}} \times C = \frac{N_{max} - N_{bound}}{N_{bound}} \times C \tag{2}$$

where N_{max} denotes the maximum amount of guest molecules that can be bound by unit weight of the material. In practical calculations, however the Eq. 2 is converted the dependence of N_{bound} against concentration as given by Eq. 3.

$$N_{bound} = \frac{N_{max} C}{K_D + C} \tag{3}$$

By fitting the experimental data both maximum bound capacity and K_D can be found. The binding constant K_D has a dimension (unit) of the concentration and the guest binding is better when K_D is smaller. In the case of our imprinted structure (thin film), it is convenient to describe the binding capacity in the units of mol·cm^{-2} rather than in mol·g^{-1} as used for bulk materials. To determine K_D values, three types of imprinted films and three types of non-imprinted films were investigated and the dependency of the amount of bound molecules as a function of the concentration of solutions for rebinding (binding isotherms) was analyzed.

As observed in Fig. 7, all imprinted films show better binding compared with their respective NI films. The important role of the PS moiety can be observed from these data, calculated binding constants, and maximum possible bound amounts provided in Table 2. First, we can confirm that the

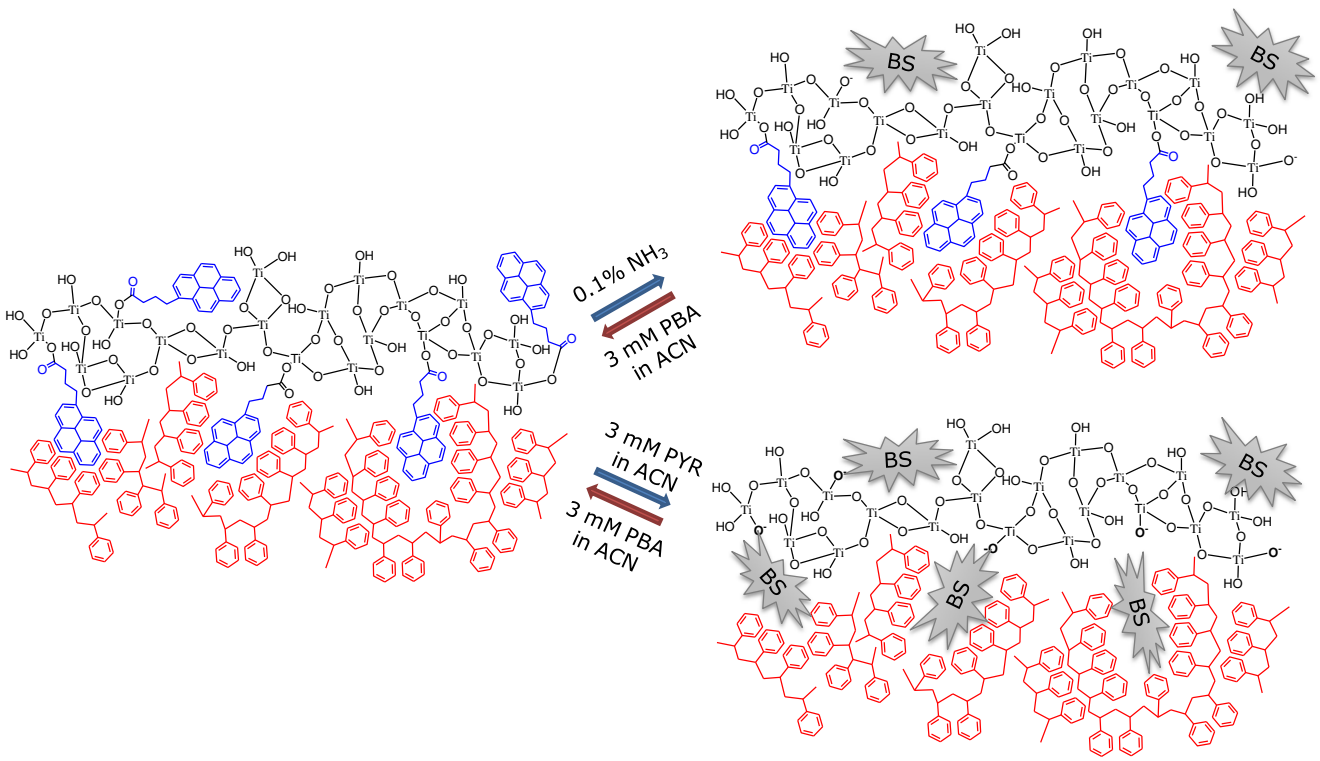

Fig. 8 Plausible mechanism of PBA imprinting in the PS/TiO_2 composite material

increase in the maximum bound capacity of the films with the PS content up to ~14 nmol·cm^{-2} is fairly good in comparison with bulk materials. If we consider the film mass, the bound capacity lies in the range of several μmol·g^{-1}; however, direct comparison with bulk materials was not performed. The best guest binding from the K_D values was obtained for the film without PS, and thus, we can notice that the binding of PBA from the lowest concentration of the binding solution (50 μM PBA in ACN) is the best in the MI-0 film. This result is consistent with previous research on carboxylic-compound-imprinted titania materials [20, 21], which demonstrated that ultrathin films of titania provide high imprinting capabilities due to surface imprinting. However, the increased thickness of titania coating decreased the permeability of guest molecules [19–24]. As expected, the imprinted films including PS showed slower guest binding than the pure titania imprinted film, especially for MI-100. Moreover, the selectivity of the films with a high PS content will probably be reduced because of higher possibilities of non-specific binding in PS, especially for molecules possessing hydrophobic moieties together with carboxylic ones.

From the above results, we can suggest that the variation in the PS content in the molecularly imprinted TiO_2/PS hybrid films is influencing the properties of the binding sites. This fact can be used to produce materials based on their expected application and whether binding capacity or binding speed is more important. The addition of PS makes the coating thicker, which in contrary to the conventional titania imprinting, increases the amount of binding sites in the material. For instance, the ca. 300-nm-thick MI-100 film was able to provide almost two times more binding sites than the pure titania imprinted film (see Fig. 4a). All initial template molecules could be completely removed and reversibly rebound. In particular, the optimized PS content can lead to the creation of sufficiently selective binding to target molecules (comparable with MI-0) with an increased capacity.

Mechanism of the template binding in the hybrid TiO_2/PS imprinted film

On the basis of the experimental results, we suggest the morphology of the hybrid imprinted matrix and two types of binding sites available in the composite material to be as shown in Fig. 8. In the fabricated material, interaction with template characteristic for imprinting with possibility of reversible binding/removal is supported by two points: one is the complexation of the carboxylic moiety of the template with the titania matrix, and the other is the π–π interaction of the pyrene moiety of the template with the PS network. As supported by experimental data, the PBA binding in the MI-100 film is different than that in the pure titania MI-0 film. In the MI-100 film, there were additionally around 20 phenyl rings of PS per molecule of the template. In such a system, the coordination of PS aromatic moieties to form a weak hydrophobic interaction with the pyrene moiety is much more probable. In the MI-20 film, such an effect is not highly pronounced but still present because of the specific phase-separated distribution of PS in composite matrix. In this case, PS domains are supposed to be the places for more concentrated binding of guest molecules.

Conclusion

In conclusion, the present study demonstrates a novel approach for molecular imprinting on the interface of specific organic/inorganic hybrid structures in nanofilms. The combination of PS and Ti(O^n-Bu)$_4$, which have been previously used to provide unique phase-separated nanostructures, can also be adapted for the biphasic imprinting of molecules possessing aromatic moieties and functional groups available for complexing with the titania matrix. The observed properties of the imprinted films are varied depending on the PS content. The maximum bound capacity was enhanced with increasing PS, indicating its role in the formation of specific binding sites, especially for the compounds possessing the pyrene moiety (1-pyrenebutyric acid, PBA) or several aligned aromatic rings (anthracene-9-carboxylic acid, 9-AC). We expect that the current approach could provide a new direction for molecular imprinting based on hybrid nanomaterials for diverse applications.

Acknowledgments This work was supported by MEXT via the 2nd Kitakyushu Knowledge-based Cluster Project. R. Selyanchyn acknowledges the Japan Society for the Promotion of Science (JSPS) for research fellowship for Young Scientists (JSPS-DC2).

References

1. Wulff G (1995) Molecular imprinting in cross-linked materials with the aid of molecular templates—A way towards artificial antibodies. Angew Chem Int Ed Engl 34:1812–1832
2. Lee SW, Ichinose I, Kunitake T (1998) Molecular imprinting of protected amino acids in ultrathin multilayers of TiO_2 gel. Chem Lett 27:1193–1194
3. Fujishima A, Zhang X, Tryk DA (2008) TiO_2 photocatalysis and related surface phenomena. Surf Sci Rep 63:515–582
4. Su C, Hong BY, Tseng CM (2004) Sol–gel preparation and photocatalysis of titanium dioxide. Catal Today 96:119–126
5. Hsu CY, Lin HY, Thomas JL, Wu BT, Chou TC (2006) Incorporation of styrene enhances recognition of ribonuclease A by molecularly imprinted polymers. Biosens Bioelectron 22:355–363
6. Yang P, Deng T, Zhao D, Feng P, Pine D, Chmelka BF, Whitesides GM, Stucky GD (1998) Hierarchically ordered oxides. Science 282: 2244–2246
7. Holland BT, Blanford CF, Do T, Stein A (1999) Synthesis of highly ordered, three-dimensional, macroporous structures of amorphous or crystalline inorganic oxides, phosphates, and hybrid composites. Chem Mater 11:795–805

8. Kartsonakis IA, Liatsi P, Danilidis I, Bouzarelou D, Kordas G (2008) Synthesis, characterization and antibacterial action of hollow titania spheres. J Phys Chem Solids 69:214–221
9. Jang IB, Sung JH, Choi HJ, Chin I (2005) Synthesis and characterization of titania coated polystyrene core-shell spheres for electronic ink. Synth Met 152:9–12
10. Wijnhoven JEGJ, Bechger L, Vos WL (2001) Fabrication and characterization of large macroporous photonic crystals in titania. Chem Mater 13:4486–4499
11. Yi J, Lu D, Li X, Hu S, Li W, Lei J, Wang Y (2012) Preparation and performance of porous titania with a trimodal pore system as anode of lithium ion battery. J Solid State Electrochem 16:443–448
12. Liu WL, Wang L, Zhang LD, Xu WH, Chen SH, Wang XQ, Duan XL (2012) Superhydrophobic surface by immobilization of polystyrene on vinyl-modified titania nanoparticles. Journal of Sol–gel. Sci Technol 62:424–431
13. Hou W, Wang Q (2009) UV-driven reversible switching of a polystyrene/titania nanocomposite coating between superhydrophobicity and superhydrophilicity. Langmuir 25:6875–6879
14. Villafiorita-Monteleone F, Canale C, Caputo G, Cozzoli PD, Cingolani R, Fragouli D, Athanassiou A (2011) Controlled swapping of nanocomposite surface wettability by multilayer photopolymerization. Langmuir 27:8522–8529
15. Mao X, Hu B, He M, Chen B (2012) High polar organic–inorganic hybrid coating stir bar sorptive extraction combined with high performance liquid chromatography-inductively coupled plasma mass spectrometry for the speciation of seleno-amino acids and seleno-oligopeptides in biological samples. J Chromatogr A 1256: 32–39
16. Mizutani N, Korposh S, Selyanchyn R, Yang DH, Lee CS, Lee SW, Kunitake T (2012) One-step fabrication of polystyrene-TiO_2 nanosandwich film by phase separation. Chem Lett 41:552–554
17. Schmidt RH, Haupt K (2005) Molecularly imprinted polymer films with binding properties enhanced by the reaction-induced phase separation of a sacrificial polymeric porogen. Chem Mater 17: 1007–1016
18. Schmidt RH, Belmont AS, Haupt K (2005) Porogen formulations for obtaining molecularly imprinted polymers with optimized binding properties. Anal Chim Acta 542:118–124
19. Ichinose I, Kikuchi T, Lee SW, Kunitake T (2002) Imprinting and selective binding of di- and tri-peptides in ultrathin TiO_2-gel films in aqueous solutions. Chem Lett 31:104–105
20. Kunitake T, Lee SW (2004) Molecular imprinting in ultrathin titania gel films via surface sol–gel process. Anal Chim Acta 504:1–6
21. Lee SW, Ichinose I, Kunitake T (1998) Molecular imprinting of azobenzene carboxylic acid on a TiO_2 ultrathin film by the surface sol–gel process. Langmuir 14:2857–2863
22. Lee SW, Ichinose I, Kunitake T (2002) Enantioselective binding of amino acid derivatives onto imprinted TiO_2 ultrathin films. Chem Lett 31:678–679
23. Yang DH, Lee SW, Kunitake T (2005) Facile fabrication of molecularly imprinted cavities in spin-coated TiO_2 nanofilms. Chem Lett 34:1686–1687
24. Mizutani N, Yang DH, Selyanchyn R, Korposh S, Lee SW, Kunitake T (2011) Remarkable enantioselectivity of molecularly imprinted TiO_2 nano-thin films. Anal Chim Acta 694:142–150
25. Komiyama M, Takeuchi T, Mukawa T, Asanuma H (2003) Molecular imprinting. Wiley-VCH, Weinheim